(2)

WL/MN-TR-91-76

Measurement of Acceleration Using an Instrumented Railgun Projectile

Donald M. Littrell
Wright Laboratory, Armament Directorate
Analysis and Strategic Defense Division
Electromagnetic Launcher Technology Branch
Eglin AFB FL 32542-5000

Keith A. Jamison, Roger D. Hudson
Science Applications Intl. Corp.
Eglin Parkway
Shalimar FL 32579

Michael J. Fernandez
U.S. Air Force 3202 Civil Engineering Squadron
Eglin AFB FL 32542-5000

Scott A. Ager
Instrumentation and Engineering Services, Inc.
Fort Walton Beach FL 32549

JUNE 1992

FINAL REPORT FOR PERIOD APRIL1990 - APRIL 1991

WRIGHT LABORATORY, ARMAMENT DIRECTORATE

Air Force Systems Command ▮ United States Air Force ▮ Eglin Air Force Base

NOTICE

When Government drawings, specifications, or other data are used for any purpose other than in connection with a definitely Government-related procurement, the United States Government incurs no responsibility or any obligation whatsoever. The fact that the Government may have formulated or in any way supplied the said drawings, specifications, or other data, is not to be regarded by implication, or otherwise as in any manner construed, as licensing the holder, or any other person or corporation; or as conveying any rights or permission to manufacture, use, or sell any patented invention that may in any way be related thereto.

This technical report has been reviewed and is approved for publication.

The Public Affairs Office has reviewed this report, and it is releasable to the National Technical Information Service (NTIS), where it will be availabe to the general public, including foreign nationals.

FOR THE COMMANDER

George F. Kirby

GEORGE F. KIRBY
Chief, Analysis & Strategic Defense Division

Even though this report may contain special release rights held by the controlling office, please do not request copies from the Wright Laboratory, Armament Directorate. If you qualify as a recipient, release approval will be obtained from the originating activity by DTIC. Address your request for additional copies to:

Defense Technical Information Center
Cameron Station
Alexandria VA 22304-6145

If your address has changed, if you wish to be removed from our mailing list, or if your organization no longer employs the addressee, please notify WL/MNSH, Eglin AFB FL 32542-5000, to help us maintain a current mailing list.

Do not return copies of this report unless contractual obligations or notice on a specific document requires that it be returned.

REPORT DOCUMENTATION PAGE

Form Approved
OMB No. 0704-0188

1. AGENCY USE ONLY *(Leave blank)*	2. REPORT DATE	3. REPORT TYPE AND DATES COVERED
	June 1992	Final, April 1990–April 1991

4. TITLE AND SUBTITLE

Measurement of Acceleration Using an Instrumented Railgun Projectile

5. FUNDING NUMBERS

C: F08635-87-C-0003
PE: 63217C
PR: 1203
TA: 03
WU: 98

6. AUTHOR(S)

Donald M. Littrell (AF program manager), Keith A. Jamison, Roger D. Hudson, Michael J. Fernandez, and Scott A. Ager

7. PERFORMING ORGANIZATION NAME(S) AND ADDRESS(ES)

Wright Laboratory, Armament Directorate
Analysis and Strategic Defense Division
Electromagnetic Launcher Technology Branch (WL/MNSH)
Eglin AFB FL 32542-5000

8. PERFORMING ORGANIZATION REPORT NUMBER

9. SPONSORING/MONITORING AGENCY NAME(S) AND ADDRESS(ES)

(same as above)

10. SPONSORING/MONITORING AGENCY REPORT NUMBER

WL/MN-TR-91-76

11. SUPPLEMENTARY NOTES

Availability of this report is specified on verso of front cover.

12a. DISTRIBUTION/AVAILABILITY STATEMENT	12b. DISTRIBUTION CODE
Approved for public release; distribution is unlimited.	A

13. ABSTRACT *(Maximum 200 words)*

An instrumented package has been accelerated in a railgun projectile to measure the inbore acceleration as a function of time. Direct, continuous acceleration profiles have been repeatedly obtained with this package during electromagnetic launch and downrange soft catch. These proof-of-principle experiments were conducted using a square bore railgun and off-the-shelf components for the *in situ* measurement, digitization, and storage of acceleration data. A continuous record of the entire launch event clearly shows gas injection, electromagnetic propulsion, and downrange deceleration in a soft catch recovery system. The launch package was subject to peak accelerations of nearly 30 kilogees (2.8 X $10^5 m/s^2$) in the electromagnetic propulsion phase of the launch. Velocity and position data obtained through integration of this data are correlated with velocity data derived from conventional static diagnostic (*e.g.*, magnetic flux loops) to validate the technique. The peak acceleration was slightly more than anticipated from the electrical current delivered to the railgun, and this deviation is examined. The paper presents a description of the experimental apparatus, acquired data, a comparison of the data with code simulations, and suggestions for future work.

14. SUBJECT TERMS	15. NUMBER OF PAGES
Railgun, Electromagnetic Launcher, Electromagnetic Acceleration	30
	16. PRICE CODE

17. SECURITY CLASSIFICATION OF REPORT	18. SECURITY CLASSIFICATION OF THIS PAGE	19. SECURITY CLASSIFICATION OF ABSTRACT	20. LIMITATION OF ABSTRACT
Unclassified	Unclassified	Unclassified	Unlimited

PREFACE

This report documents a study of acceleration in an electromagnetic railgun using an instrumented projectile named In-Bore Instrumented/Diagnostics (IBID). This paper was presented at the Third European Symposium on Electromagnetic Launcher Technology in London, England on 16-18 April 1991; it was originally published in the proceedings of that conference and is reproduced here due to the limited distribution of that publication.

This work was funded by the Wright Laboratory, Armament Directorate, Strategic Defense and Analysis Division, Electromagnetic Launcher Technology Branch (WL/MNSH) under the Kinetic Energy Weapons program of the Strategic Defense Initiative. Personnel from Wright Laboratory and Science Applications International Corporation (SAIC) performed the work during the period April 1990 to April 1991 at Eglin Air Force Base FL 32542. This effort was partially funded under contract F08635-87-C-0003.

TABLE OF CONTENTS

FIGURES

TABLES

ABBREVIATIONS AND ACRONYMS

μV/gee	microvolt per gee
A/D	Analog to Digital
cm	centimeter
DC	Direct Current
EM	Electromagnetic
EML	Electromagnetic Launcher
EMP	Electromagnetic Pulse
ET	Electrothermal
Hz	Hertz
IBID	In-Bore Instrumentation/Diagnostics
kA	kiloamp
kg	kilogram
kgee	kilogee
kHz	kilohertz
kJ	kilojoule
km/s	kilometer per second
m/s	meter per second
m	meter
MHz	Megahertz
mm	millimeter
V	Volt

SECTION I

INTRODUCTION

The in-bore projectile environment has been identified by electromagnetic launcher (EML) projectile designers as a key technical issue (Reference 1). This environment is defined by acceleration, jerk, magnetic and electric field intensities as well as transient field effects. Very few details of the projectile environment have been verified although several conditions are expected to be rather harsh. The exact acceleration of an EML projectile is somewhat difficult to accurately predict due to the complex combination of electrical, magnetic, mechanical, and thermal forces. Improved techniques to provide high resolution measurements of the acceleration, velocity, and position histories of projectile motion are needed for the development and validation of predictive in-bore ballistics codes and the design and optimization of high performance projectiles.

Thus far, the search for accurate, high resolution measurement techniques of EML projectile acceleration has proved to be elusive. Historically, B-dot probes are the most popular position versus time measurement devices in electromagnetic guns. Like all distance-time measurements, differentiation is required to obtain velocity-time histories, and a second differentiation to obtain acceleration-time histories. Due to limitations in the number of probes and uncertainties in data reduction, the acceleration deduced by double differentiation usually lacks the accuracy desired by the researcher.

Several techniques have been attempted to directly measure velocity as a function of time; most have had no or only limited success. The railgun flux loop technique (Reference 2) requires high resolution digital data recording (10 bits or greater) and is constrained to constant current railgun accelerations to obtain good results. Techniques such as Doppler radar microwave, visible, infrared, and laser interferometry (Reference 3 and 4) suffer from signal loss caused by plasma blow-by, a cloud of debris, or a shock front traveling in front of the projectile.

The detection, storage, and retrieval of acceleration data by an on-board electronics package is appealing for two reasons. First, it provides information on the actual performance of a launcher, and second, it signals the beginning of an effort to equip EMLs with "smart" projectiles. The measurement of projectile motion with an on-board accelerometer has been documented by researchers at Boeing (Reference 5 and 6) and Parker Kinetic Designs (PKD)/Army Research and Development Engineering Center (ARDEC) (Reference 7). In both instances, an on-board accelerometer was linked to an out-of-bore recording device via connecting wires. Advantages over the autonomous recording package include: lower projectile mass for greater accelerations, no soft catch requirements to limit the study of target effects/interactions, and reduced hardware requirements for simplicity of design and lower cost. The limitations of this technique are a restricted positional range and unwanted electrical noise induced in the connecting wires.

Interpretation of this data is hampered by the non-constant mass of the payload as the connecting wires are pushed down the bore by the projectile. Table 1 is a brief summary of test conditions and pertinent data from these experiments.

TABLE 1. ACCELEROMETER TEST SUMMARY

Test Conditions	PKD	BOEING	IBID197	IBID235
Maximum current (kA)	550	150	821	941
Distance traveled (m)	<1.3	<0.18	>7	>7
Injection velocity (m/s)	---	0	149	162
EML velocity (m/s)	<300	---	264	360
Injector acceleration (kgee)	18	N/A	3.5	3.5
EML peak acceleration (kgee)	12	15	20	28
Projectile mass (kg)	---	---	1.17	1.15
Kinetic energy (kJ)	---	---	48	74
Bore size (mm)	50	25	51	51
Armature type	---	---	plasma	plasma

SECTION II

EXPERIMENTAL HARDWARE/APPARATUS

The launch package, pictured in Reference 8, consisted of a sabot, an armature, an electronics package, and a containment vessel for structural protection and electromagnetic shielding of the electronics.

The sabot was a one-piece structure fabricated of lexan. Its multiple functions were as follows: (1) electrically insulate the electronics from the rails, (2) serve as a pusher plate for the electronics containment tube, (3) serve as a mounting surface for the armature, and (4) seal the bore against plasma arc blow-by. The plasma armature was formed through vaporization of an hourglass-shaped aluminum fuse (Reference 9) attached to the rear face of the sabot. The hourglass-shaped fuse is designed to "soften" plasma arc initiation by extending the vaporization time. This design was chosen to mitigate any sharp transients in acceleration that might accompany the violent explosion of the rapidly vaporizing fuse.

An aluminum containment vessel had the dual role of shielding the electronic components from Electromagnetic Pulse (EMP) and providing structural protection of the electronics during deceleration. The electronic cavity in the right circular cylinder was accessed via a threaded cone-shaped nose. The nose cone in these tests was fabricated of aluminum; yet, the design allows more dense materials to be substituted if a forward shift in the center of gravity is needed for downrange aerodynamic stability.

The on-board electronics package incorporates four components: an accelerator, an analog recorder with built-in computer interface port, a battery pack, and a g switch to trigger the recorder. All components are commercially available. Because of an emphasis on concept demonstration, this program focused on the packaging of existing commercial hardware rather than the development, integration, and optimization of new electronics. This approach entailed a substantial mass penalty and obvious restrictions in size since no miniaturization of components was attempted. The physical dimensions of the apparatus mandated the use of a large-bore EML (Reference 10) with an appropriately sized power supply.

Piezoresistive accelerometers specifically designed for high g applications were selected for these tests. These accelerometers feature such characteristics as low impedance, high overrange, zero damping, and an exceptionally high resonant frequency. These latter two attributes allow the accelerometers to respond accurately to the fast rise time, short duration shock motion found in EMLs.

The recording instrument was a one channel, 8-bit analog recorder (IES Model 31) rated for high (100,000) g applications (Reference 11). It was originally developed to measure the in-bore ballistic behavior of conventional artillery and to collect environmental data during projectile impact. The theoretical lower limit for sampling, set by the Shannon sampling theorem, is two samples per filter cutoff frequency; at least five samples per cycle are recommended for most applications. Per specification, the recorder was factory-set at a 2 MHz sampling rate and a Direct Current (DC) to 131 kHz signal bandwidth with a 4-pole Butterworth filter. The standard recorder was equipped with an expanded memory option that extended the memory size to 128 kilobytes (65 milliseconds) and the pre-trigger data storage to 7138 bytes. The recorder was encapsulated in potting compound inside a right circular cylinder with a diameter of 25.4 mm length of 57.4 mm, and weighed 57 grams.

The recorder was activated by an impact switch or g switch (Aerodyne Controls) designed to trigger at a low acceleration level. It was powered by six 1.5 volt cells from a standard 9 volt alkaline battery (Duracell Model MN1604B) connected in series and encapsulated in potting compound. See Reference 11 for details on battery encapsulation procedures. The recorder, batteries, and accelerometer were encased in steel shells for structural support and for EMP shielding.

SECTION III

MEASUREMENTS

Two test, designated as IBID197 and IBID235, were conducted as proof-of-principle demonstrations of the on-board accelerometer concept. The data collected from these tests are shown in Figures 1 and 2. For clarity, the data traces are shown both in the raw state and after digital filtering at 12 kHz.

The data show four distinct phases of acceleration: (1) a relatively low magnitude, prolonged period of acceleration in the light gas gun injector, (2) a short intense period of electromagnetic acceleration, (3) flight through the gun after current decay followed by free-flight after exiting the barrel, and (4) staged deceleration in a soft catch device.

For IBID197, controlled deceleration of the projectile was accomplished via passage through lightweight foam and plywood stacked perpendicular to the lime of flight in alternating layers. The acceleration profile (Figure 1) shows a number of discrete deceleration events corresponding to each plywood layer. As expected, the general trend of the deceleration profile is a decrease in frequency and in magnitude of these events as the velocity of the projectile falls. The deceleration history of IBID235 (Figure 2) differs from IBID197 due to the addition of a sandbag in the soft catch tank to compensate for the increased kinetic energy. The objective of the second test was to replicate the results of the first. The important differences in the two tests were the change in soft catch materials, a slight dissemblance in EML acceleration level stemming from the input current magnitude (941 kA for IBID235 versus 821 kA for IBID197), and a variance in resolution of the two recorders. The signal-to-noise ratio is dependent upon amplifier gain, accelerometer sensitivity, and the magnitude of acceleration. The accuracy of the data is affected by the sample rate and the g's per bit value. Since the acquisition rate (2 MHz sampling) is fast in comparison to the bandwidth (131 kHz), the g's/bit value is the dominant factor for obtaining high resolution measurements. Most integration errors occur during the free flight of the projectile in which the magnitude of acceleration or deceleration is low and fairly constant over a long period. The g's/level value is determined by the gain of the recorder amplifier and the sensitivity of the accelerometer (see Table 2). If higher acceleration/deceleration peaks are to be recorded, the amplifier gain must be reduced; this increases the g's/bit value, thus reducing the resolution of the data, and introduces more error in the integration. Conversely, lowering the g's/bit calibration value increases integration accuracy but reduces the acceleration-deceleration range.

In sampled data systems, the signal bandwidth must be limited to less than half the sampling frequency to avoid data corruption by aliasing. This is particularly true for this sensor as it has a noise amplitude characteristic that rises continuously with frequency. To define the required

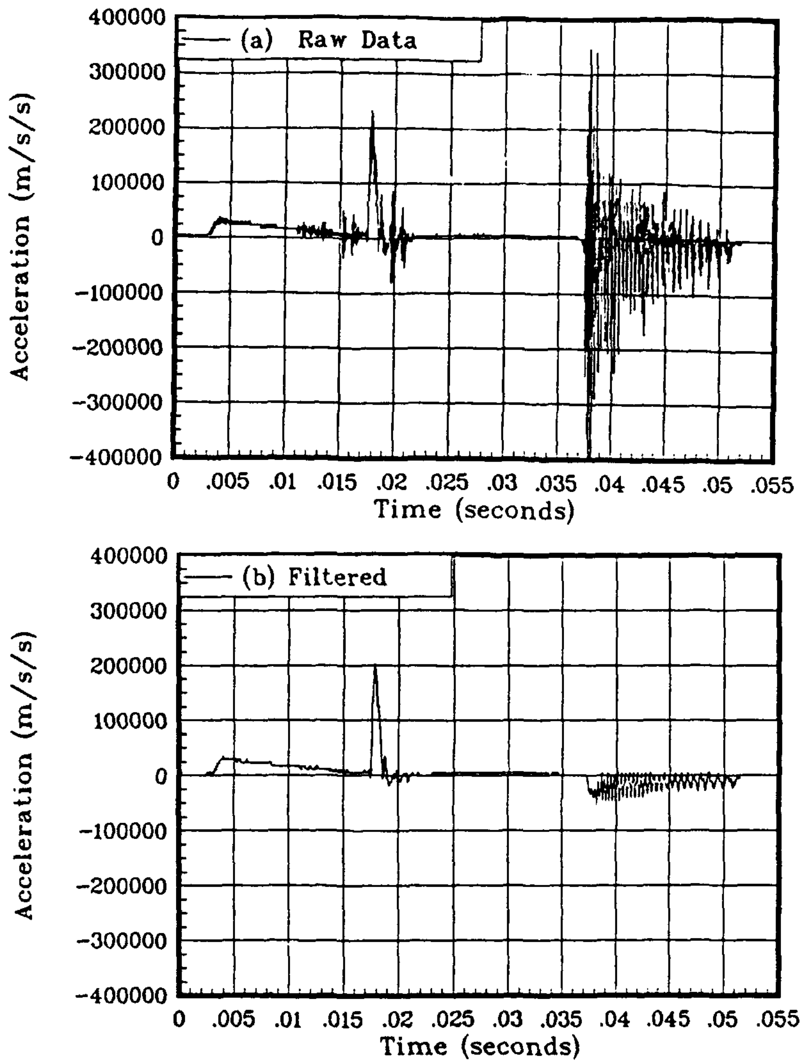

Figure 1. IBID197 Acceleration Record, (a) Raw Data and (b) Filtered Data

bandwidth for monitoring the acceleration, a sampling rate believed significantly to exceed the requirement was used. The recorder low pass cutoff frequency was 131 kHz. By applying digital filtering techniques, the bandwidth can be reduced as necessary. Due to the increase of noise with frequency, an artifact will always be seen riding the signal excursion. This artifact takes the form of an oscillation at a frequency just below cutoff; it should be ignored. The selection of post-shot filtering frequency is somewhat arbitrary, although it is intended to eliminate some information that may not correspond to whole body acceleration. The accelerometer and associated electronics were enclosed in a launch package 22 cm long. Assuming that sound speed in the launch package

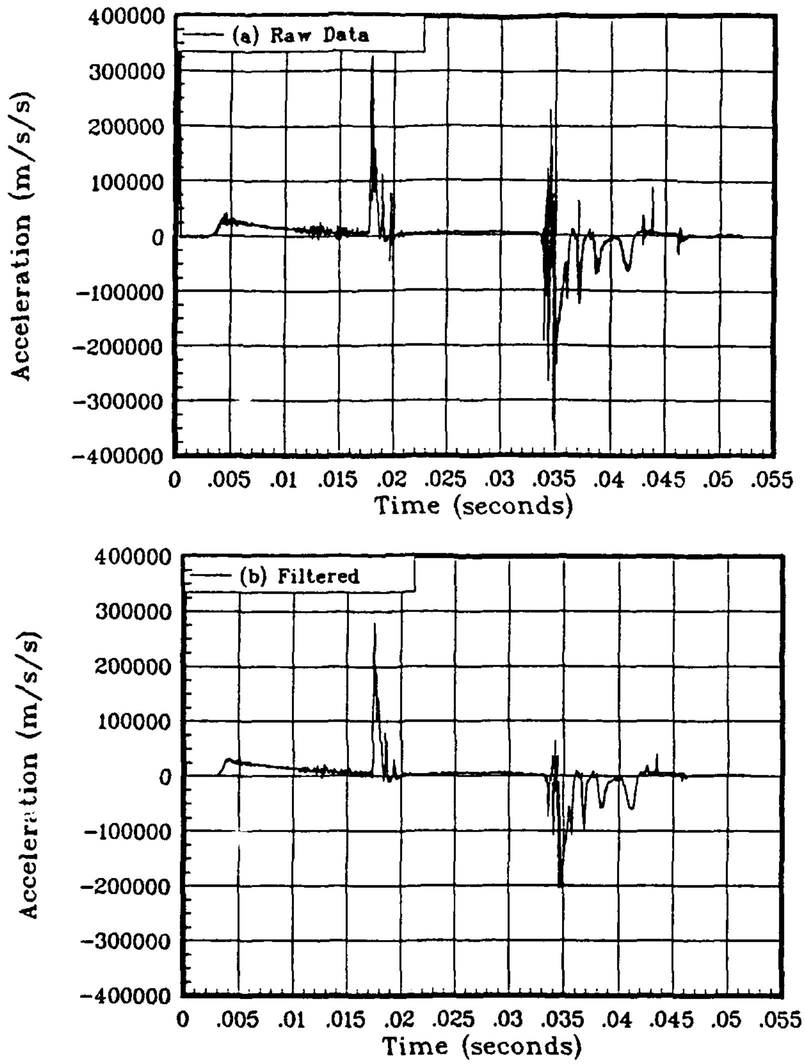

Figure 2. IBID235 Acceleration Record, (a) Raw Data and (b) Filtered Data

is on the order of 5 km/s, then events with frequencies higher than 10 kHz probably do not represent whole body acceleration. Components within the launch package can oscillate at higher frequencies but such vibrations are not of interest here. Typically, the 12 kHz filtering results in a data set that is easier to interpret.

As Table 2 shows, the second test, IBID235, offers better resolution due to the higher overall gain; thus, the majority of the data analyses are accomplished on these data.

TABLE 2. DATA COLLECTION SPECIFICATION

Shot Designation	IBID197	IBID235
Date	7/16/90	8/23/90
Sample rate (MHz)	1.9183	1.9157
Sample period (microseconds/pt)	0.5231	0.5220
Accelerometer range (kgees)	60.	200.
Accelerometer sensitivity (μV/g)	1.57	1.17
Amplifier gain	21.14	57.39
Amplifier offset (V)	2.656	2.676
Resolution (g's/bit)*	588.55	290.90

* The amplitude range is divided into 256 discrete levels for an 8-bit Analog to Digital (A/D) with a 5 volt range.

SECTION IV

DISCUSSION OF RESULTS

The measured acceleration profiles contain information about the operation and performance of the railgun (Reference 10). While the railgun was operated far below its full capacity for these tests, the data still provides insight into the behavior of railguns as macro particle accelerators. This section presents considerations for data validation, a comparison of the measured acceleration to two simulation codes, a discussion of some unanticipated features in the acceleration profiles, and predictions of the payload environment.

1. VALIDATION TECHNIQUES

Perhaps the most straightforward method of data validation is the direct comparison of the observed acceleration to that predicted by a simulation code. During the injection phase of the launch, the projectile is driven by an expanding column of helium gas from a reservoir via a fast acting valve. A simple simulation code has been written that models the projectile acceleration assuming adiabatic expansion of the gas and a Lagrange velocity gradient to account for the speed of sound in helium. The valve opening time has been measured at approximately 1.5 milliseconds and the simulation code assumes that reservoir pressure increases linearly in that time. Typically, the simulation slightly overpredicts the observed velocity of the injection system; this result is expected because friction between the projectile and bore is not accounted for properly. The predicted velocities have been within a few percent of the observed velocities for a wide range of projectile masses. Figure 3 matches the measured acceleration with the predicted acceleration from the gas gun simulation code. The time scale of the simulation has been arbitrarily offset so that the data and prediction begin at approximately the same time. Figure 3 shows good agreement between the simulated and measured values, although the simulation slightly overestimates the acceleration between 0.005 and 0.011 seconds. The electromagnetic acceleration that occurs between 0.017 and 0.020 seconds is, of course, not predicted by the gas gun simulation. Generally, this analysis qualitatively and quantitatively validates the data and illustrates that the recorder is accurate even when operating well below the maximum range setting.

In an alternate approach to data validation, the recorded data is integrated to produce a continuous velocity profile for the launch event. A second time integration produces a position versus time history. Simple numerical integration is, however, quite sensitive to the baseline or zero level of the recorded data. Figure 4 displays both the single and double integration of the acceleration recorded for IBID235. The electromagnetic acceleration is seen as a dramatic rise from 200 to 340 meters/second at 0.018 seconds. The data suggests that the electromagnetic boost occurred after the projectile had traveled approximately 2 meters from its initial position. This result validates the doubly integrated data during the gas gun portion of the acceleration. The deceleration (when the projectile struck the plywood in the soft catch system) should have occurred at 7.9 meters. There is strong evidence in the data that this deceleration began at 0.034 seconds at very nearly the correct position. Again, the close agreement between the integrated data and the physical arrangement of the experiment adds credibility to the data.

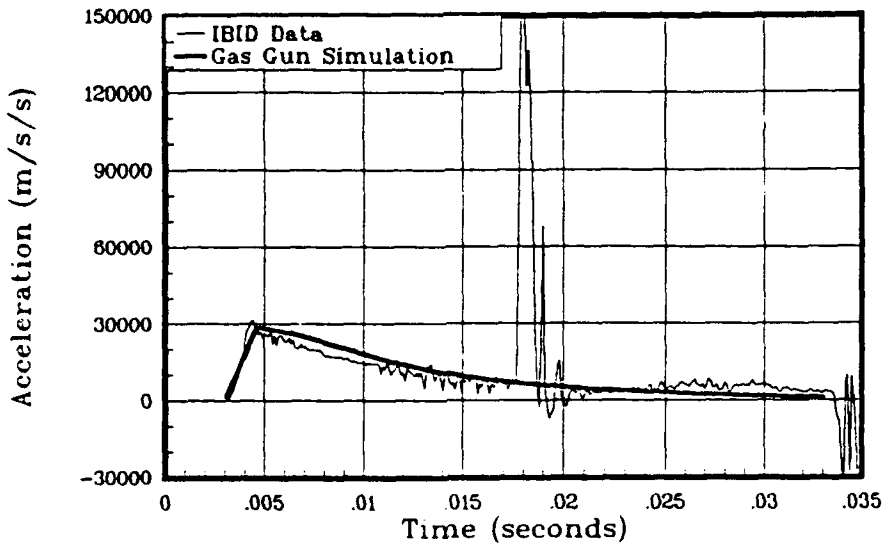

Figure 3. Comparison of IBID235 Acceleration with Gas Gun Simulation

Deceleration is evident in the velocity history between 0.034 and 0.042 seconds. The projectile came to rest approximately 9.5 meters from its initial starting location. The failure of the velocity integral to return to zero is of some concern but a number of potential problems may have occurred. First, the amplified baseline may have shifted slightly during the event with the error being compounded by integration. Second, the accelerometer may have been overdriven or changed characteristics slightly during the very rapid deceleration that occurred as the projectile penetrated the sand bag in the soft catch system. Lastly, the effects of electromagnetic interference cannot be ruled out as possibly adversely effecting the measurement. The possibility of electromagnetic interference with the baseline is supported by the unexplained increase in velocity after the electromagnetic boost was complete (i.e., 0.020 to 0.034 seconds).

The final data validation technique is the comparison of the continuous velocity measurement with velocity measurements made at discrete points along the launcher as shown in Figure 5. Numerous probes are embedded along the length of the railgun and injector. These probes sense the arrival time of the launch package. The distance between the locations of adjacent probes divided by the difference in projectile arrival times yields an average velocity for the time when the projectile was between the probes.

Two types of probes are utilized to obtain discrete velocity data. First, "light gates" in the injector flight tube sense the passage of the launch package by interruption of light beams that traverse the bore. One pair of these probes is installed in the injector at a distance 0.86 meters from the breech end of the rails.

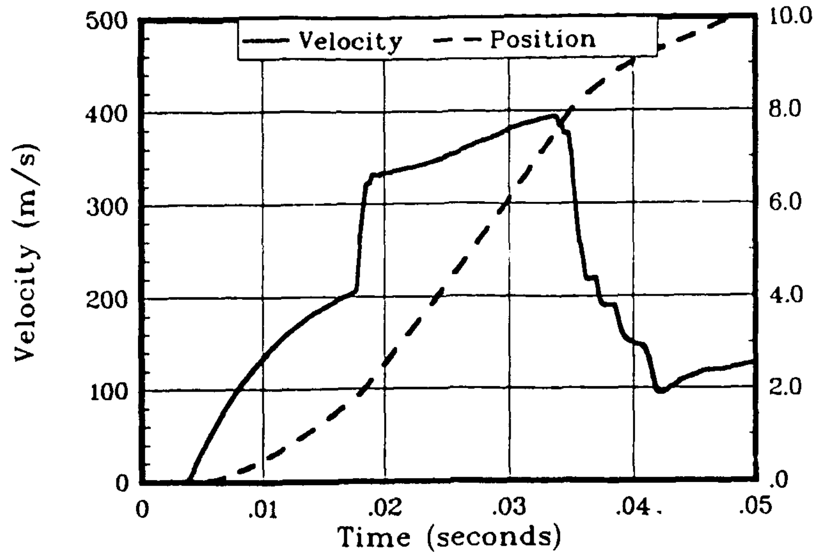

Figure 4. Velocity and Position versus Time Obtained via Integration of IBID235 Data

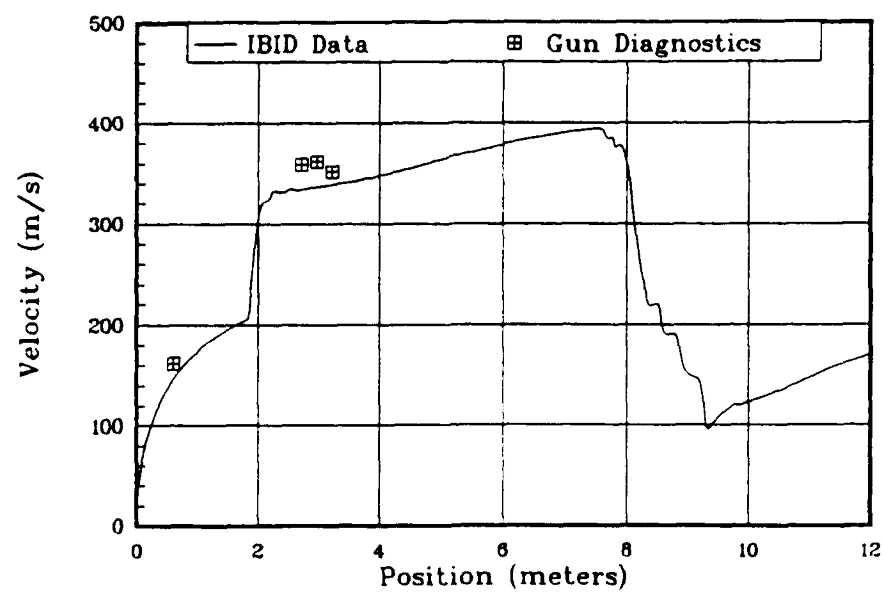

Figure 5. Comparison of Velocity Measurement Techniques for IBID235

Second, several "B-dot loops" are embedded in the insulators that separate the rails. There are three possible orientations of the B-dot loops; the probes used here are oriented to sense only magnetic field from the armature so a bipolar signal is observed when the armature passes each probe. The peak of the first portion of the signal corresponds to the leading edge of the armature or trailing edge of the projectile. Again, the difference in timing of the signals from adjacent probes was used to calculate an average velocity. The discrete velocity points may be compared directly to the continuous velocity profile if the time scales of the two recording devices can be properly correlated. Alternatively, the velocity data may be plotted as a function of probe location with respect to the initial position of the projectile. The velocity and position integrated data may then be plotted with position (projectile travel) as the ordinate and with velocity as the abscissa.

In Figure 5 the velocity is displayed as a function of distance traveled by the projectile for IBID235. The curve is the first time integral of the acceleration data plotted as a function of the double integration of the data. The discrete points are based on velocities from probe pair differences plotted at a position midway between the pair. The data point at 0.6 meters is the measured velocity in the injector flight tube, and the three data points between 2.5 and 3.5 meters are obtained from differences of four B-dot signals. Again, the independent measurements support the IBID data. Uncertainty in each of the discrete velocity measurements is between 5 and 10 percent.

2. ELECTROMAGNETIC ACCELERATION PROFILES

The total duration of the current pulse supplied to the railgun was just over three milliseconds in length with a peak value of 941 kA. The pulse width at half maximum, however, was less than one millisecond. Given the measured current profile, the ideal railgun acceleration is given by

$$a(t) = \frac{L'}{2m} [I(t)]^2 \cdot \qquad (1)$$

A direct comparison of the measured and ideal acceleration on IBID235 is shown in Figure 6 for the time window between 0.017 and 0.020 seconds. The solid curve exhibiting considerable structure is the measured acceleration. The curve labeled "Ideal Acceleration" is calculated from Equation 1 and the measured current.

The curve labeled "Electrothermal (ET) Thrust" in Figures 6 and 7 is a postulated acceleration that might occur from heating the gas behind the projectile by the ohmic dissipation in the armature. This curve is simply the product of muzzle voltage and current, which has been scaled by an arbitrary constant. Curiously, this scaling factor is about 5000 and has units of meters per second, approximately the speed of sound in the plasma armature. Subtracting the calculated electromagnetic acceleration from the measured acceleration yields the final curve labeled "Difference." Clearly, the postulated ET acceleration does not match the structure (Labeled 1 through 6) of the unanticipated acceleration.

Similar features are seen (Figure 7) for the measured, calculated, and unanticipated acceleration of IBID197. Most of the features appear to have been reproduced in both shots. In IBID197, however, the amplifier gain was not as large as in IBID235 so some features are not as clear.

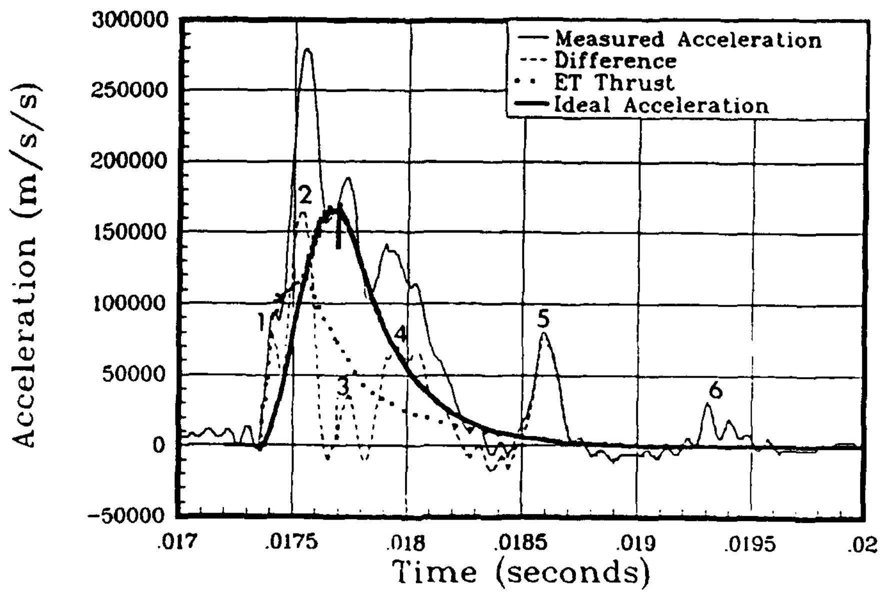

Figure 6. Comparison of Measured and Ideal Acceleration for IBID235

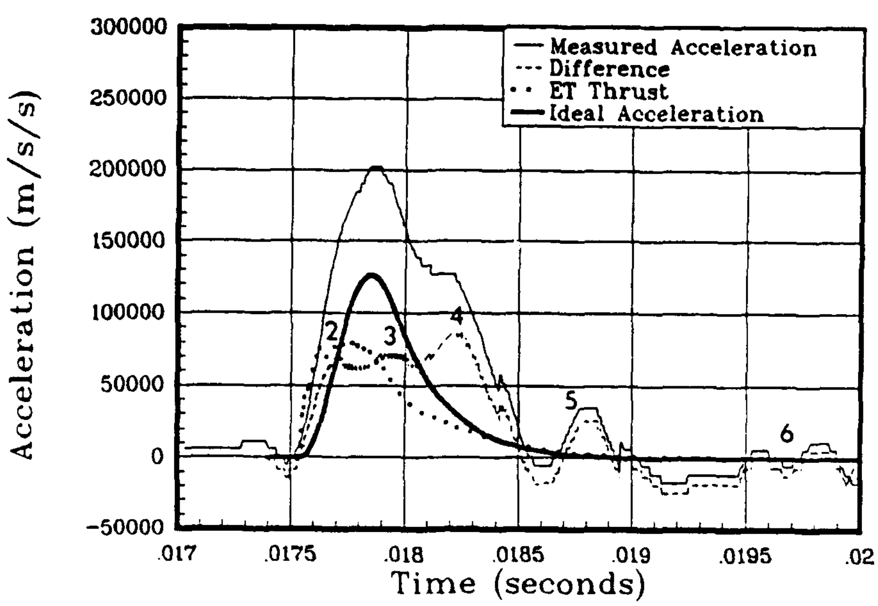

Figure 7. Comparison of Measured and Ideal Acceleration for IBID197

Feature 1 occurs 30 to 50 microseconds after current is initiated in the railgun. Examination of the breech voltage trace shows this feature to be coincident with the vaporization of the aluminum fuse. The plasma armature was formed by exceeding the action for vaporization of an hourglass-shaped fuse attached to the rear face of the launch package. It is possible that Feature 2 is related to the ET acceleration postulated above; however, the shape is not a good match, and the selected scaling factor is purely arbitrary. Feature 3 is unexplained.

The acceleration recorded during the current pulse is quite complex, but it can be decomposed into more understandable terms. The first step was to model the acceleration expected due to the current via the Lorentz force (Figure 6). The "Difference" trace in Figure 6 displays a high frequency oscillation characteristic of the type of accelerometer as discussed under filtering. A 5 kHz, low-pass filtered version (Figure 8) displays the pulsing nature of the signal, apparently riding on a decaying longer pulse. The longer pulse (trace labeled "Thermal") fits reasonably well with the thermal energy of the exploding foil fuse that initiates the plasma armature.

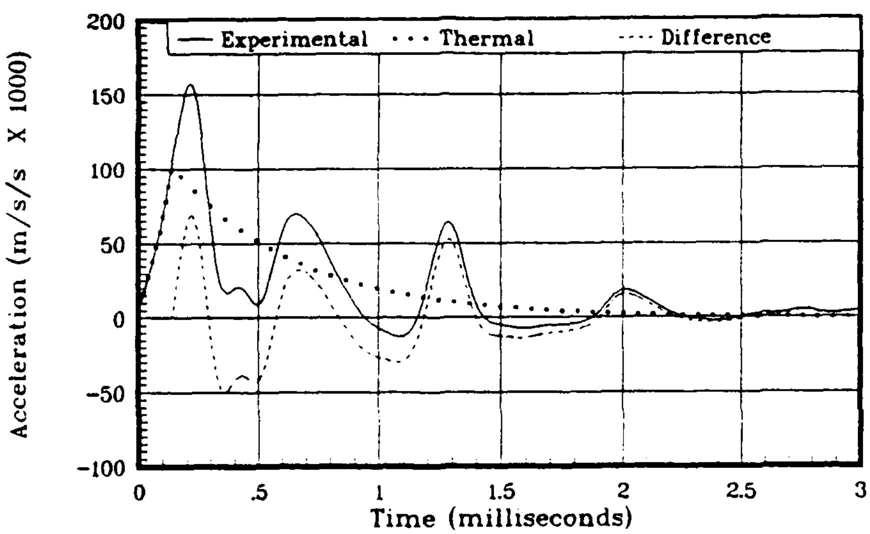

Figure 8. Possible Components of Acceleration from IBID235

In Figure 6, Features 4, 5, and 6 have a periodic spacing of approximately 640 microseconds, or equivalently, a 1.6 kHz frequency. Feature 4 is spaced 66 microseconds from current initiation. Note that the magnitude/amplitude of these peaks is decreasing with time--i.e., Feature 5 is smaller than Feature 4, and Feature 6 is smaller than Feature 5. Three possible explanations are offered: (1) the explosion of the foil creates a shock wave that repetitively passes from the projectile to the breech end of the gas injector and back again, (2) the explosion of the foil creates a shock wave that reverberates in the projectile package, or (3) the shock wave from the foil vaporization is driven repeatedly back to the projectile by magnetic forces. The first explanation is compromised by experimental evidence; in other plasma armature tests in which a pressure transducer was mounted at the breech end of the injector, no such shock waves resulting from arc initiation were observed. If the second explanation is correct, the acceleration is unique to the package and does not accurately portray the acceleration history of the projectile. This may be the source of the errors obtained in the integrated velocity and position traces (see Figures 4 and 5). For the third explanation, the "Difference" (Figure 8, dashed curve) is highly reminiscent of the constant evolution of projectile acceleration for the arc armature initiation behavior predicted by Batteh et al. in Reference 12.

3. BORE ENVIRONMENT

The presence of electromagnetic fields (B) with high rates of change (B-dot) differentiates the in-bore environment of EMLs from conventional guns. The magnetic field B at the back of the armature is estimated to be on the order of 10 Tesla for the reported tests. Fields of these strengths are high enough to influence the proper functioning of magnetic field-sensitive electronic components through the Hall effect. Fortunately, field strength in front of the armature is greatly reduced. The magnetic field strength and the time rate of change are at maximum intensity nearest the armature. Their magnitude decreases with distance from the armature, shown in Figures 9 and 10. The region of space occupied by the payload has two contributors to the magnetic field during acceleration--that produced by the armature current and that by the rail current. The directions of the B-fields produced by these two current elements are in opposition, with the rail current contribution dominating at distances very close to the armature and the influence of the armature field growing with distance from the armature. Figures 9 and 10 were generated with the current and rate of change of current (dI/dt) measured during IBID235 using a code (Reference 13) to calculate the total flux density at a specified point ahead of the armature. The locations given in the legends of Figures 9 and 10 cover the region of space where the payload was located within the launch package. Effects of these field intensities on the electronics are unknown but do not appear to be highly detrimental.

J. Asay et al. has suggested (Reference 14) that the time-changing magnetic field can induce electrical currents in coupled conductor loops or into conducting bodies of extended dimensions resulting in perturbation or burnout of electronics, and that magnetic pressure may deform metallic parts. Several steps were taken to minimize the effect of the time-changing magnetic field on the payload: (1) the plane of the recorder's circuit board was oriented orthogonal to the direction of armature current (Reference 8) to reduce the induced voltage on circuit loops, (2) the payload was designed with the sensitive circuits of the recorder positioned far from the armature in a low transient region (Figure 10), and (3) the electronics were encased in both stainless steel and aluminum conducting shells to shield sensitive circuitry.

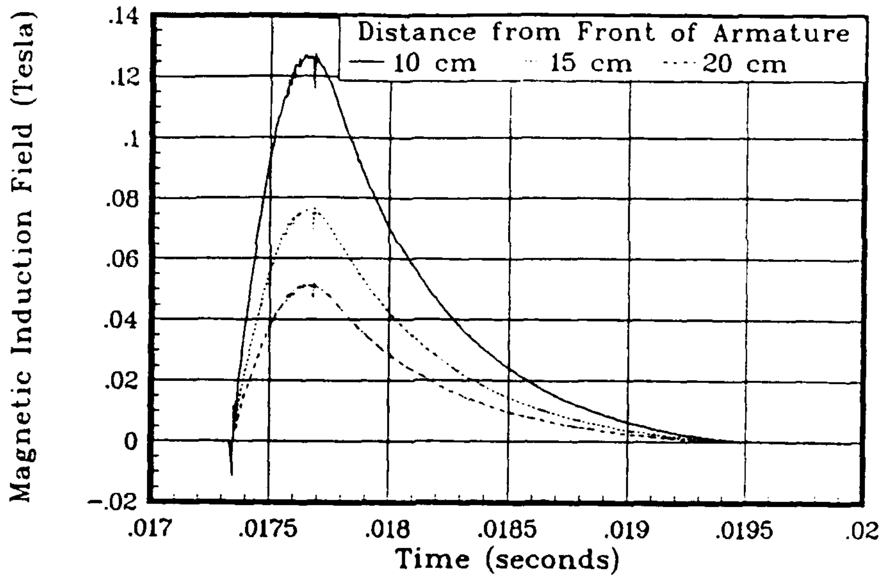

Figure 9. Calculated Magnetic Field Intensity for IBID235

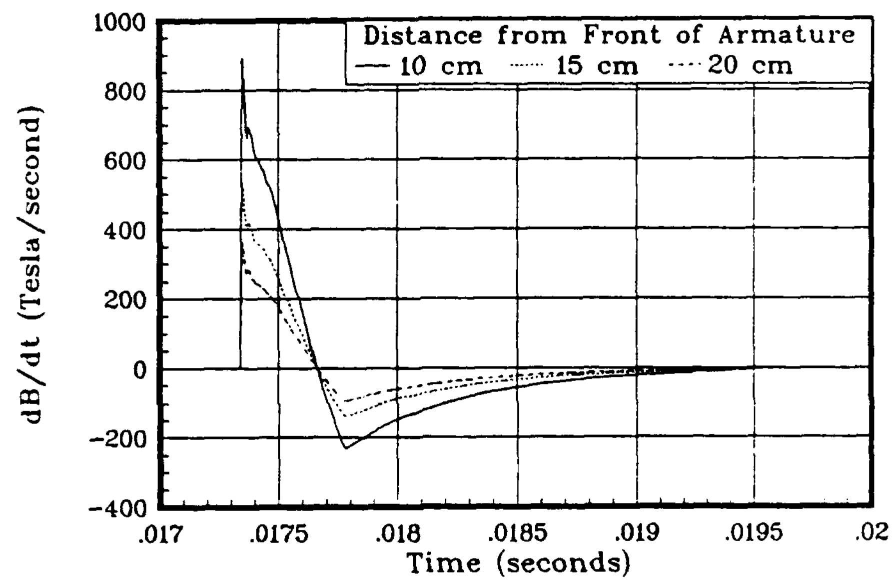

Figure 10. Calculated Time Rate of Change of Magnetic Field Intensity for IBID235

SECTION V

CONCLUSIONS AND RECOMMENDATIONS FOR FUTURE WORK

Clearly visible in both measured acceleration profiles are light-gas gun injection, electromagnetic acceleration, and deceleration in the soft catch system. The light-gas gun injection and deceleration data are readily explained by simple models. The electromagnetic acceleration revealed far more information than was anticipated. It is evident from comparison of the data and acceleration models that the formation of a plasma armature is an important event in the launching of a projectile. Three plausible explanations have been offered to account for the unexpected acceleration at the on-set of electrical current in the railgun. These effects warrant further study.

It appears that a 50 kHz bandwidth, requiring sampling (given reasonable filter parameters) at 300 kHz, is sufficient for this task. Three channels would allow x, y, and z monitoring and could be obtained by multiplexing the present recorder input. A much more difficult problem is the need for much greater resolution while maintaining range. While a 12-bit A/D converter would suffice, no 1 MHz monolithic 12-bit A/D converter has been built in the small packages required, and the technology is not expected to reach that point for several years. Compression techniques would allow the benefits of 12-bit resolution at low values, at the expense of increased error at higher values--all from an 8-bit converter.

This approach has revealed two inherent disadvantages: a requirement for a soft-catch capability, and, for small bore guns, a substantial mass penalty to carry the electronics package. A short-term solution to the first problem is structural reinforcement of the projectile to protect the electronic components during soft catch; however, this approach compounds the second problem by adding mass to the projectile. In the long term, the requirement for a soft-catch device can be eliminated through telemetry, and reductions in projectile mass will come through advances in materials and electronics packaging technologies.

Because existing laboratory hardware allows only modest increases in kinetic energy, the concept of this technique as a "flying laboratory" for other diagnostics will be exploited. While the axial acceleration of a projectile in an EML should be predictable and verifiable via conventional position-time diagnostics, balloting or the lateral motion of a projectile in a gun tube is not. An accelerometer oriented to measure lateral motion might be used to quantify the magnitude of in-bore balloting and tip-off (the effect of random lateral impulses on a projectile at bore exit due to balloting or loss of support). If size and mass restrictions imposed by the experimental EML system can be met, a multichannel recorder will be used to obtain the simultaneous measurement of axial acceleration and lateral acceleration in both the rail-to-rail and insulator-to-insulator directions.

While the data from the first two in situ tests of projectile acceleration are insufficient to reach formal conclusions about arc initiation, they clearly indicate the productivity of this method. Valuable indications of underlying mechanisms have been seen, indicating the value of this technique. The arc initiation can be studied with present capabilities, while hypervelocity arc studies must await the development of a hypervelocity soft-catch or transponder capability.

REFERENCES

1. Launch Package and Projectiles for Electric Guns, 17-19 May 1989 Workshop, Volume 1, Summary Report and Unclassified Presentations (ARDEC sponsored workshop).

2. D.P. Bauer and J.P. Barber, "In-Bore Railgun Projectile Velocity," IEEE Transactions on Magnetics, 22(6), pp. 1395-1398, November 1986.

3. W.M. Isbell and M. Koops, "Interferometric In-Bore Measurements of Electromagnetically Launched Projectiles," presented at the 41st meeting of the Aeroballistic Range Association, San Diego, California, October 1990.

4. R.S. Hawke, J.R. Asay, C.A. Hall, R.J. Hickman, C.H. Konrad, J.L. Sauve, and A.R. Susoeff, "Armature Formation in a Railgun Using a Two-Stage Light-Gas Gun Injector," IEEE Transactions on Plasma Science, 17(3), pp. 378-385, June 1989.

5. Jeff Thoman, "Rail Gun Material Survey Summary and Launch Environment Simulator Description," 2nd Electromagnetic Launcher Association meeting, Pomona, California, July 1986.

6. Jeff Thompson, "Component Testing and Launch Environment Diagnostics," 3rd Electromagnetic Launcher Association meeting, Tamarron, Colorado, March 1987.

7. Robert G. Grzesik, David E. Mitchell, James H. Sebastian, Ing Woo Chin, and Steven A. Kostakis, "E/M Launcher Vibration and Acceleration Data Analysis," IEEE Transactions on Magnetics, 27(1), pp. 147-151, January 1991.

8. M.J. Fernandez, S.A. Ager, and R.D. Hudson, "In-Bore Instrumentation/Diagnostics for Large-Bore EMLs," IEEE Transactions on Magnetics, 27(1), pp. 185-188, January 1991.

9. K.A. Jamison and D.M. Littrell, "A Technique to Reduce Plasma Armature Formation Voltage," IEEE Transactions on Magnetics, 27(1), pp. 318-322, January 1991.

10. M.M. Holland, G.M. Wilkinson, A.P. Krickhuhn, and R. Dethlefsen,, "Six Megajoule Rail Gun Test Facility," IEEE Transactions on Magnetics, 22(6), pp.1521-1526, November 1986.

11. "User Manual, Model 31 Recorder," Instrumentation and Engineering Services, Inc., May 1990.

12. Jad H. Batteh, G.E. Rolader, J.D. Powell, and Prateen V. Desai, "A Time-Dependent Model for Railgun Plasma Armatures," Physics of Fluids, 31(6), p. 1757, June 1988.

13. L.D. Thornhill, J.J. Scanlon, and J.H. Batteh, "Determination of Jerk, Acceleration, and Magnetic Field Loading on a Projectile Launched from an Electromagnetic Railgun," Wright Laboratory, Armament Directorate, technical report to be published.

14. J. Asay et al., Projectile Panel of the Diagnostics Techniques Workshop, Proceedings of the Electromagnetic Launcher Workshop II-Diagnostic Techniques, AFATL-TR-87-65, Air Force Armament Laboratory, Eglin AFB FL 32542-5000, pp. 37-39, January 1988.

Distribution
WL/MN-TR-91-76

Defense Tech Info Center
Attn: DTIC-DDAC
Cameron Station
Alexandria VA 22304-6145
2

AUL/LSE
Maxwell AFB AL 36112-5564
1

AFCSA/SAMI
The Pentagon, Room 1D363
Washington DC 20330-5425
1

Eglin AFB FL 32542-5000

WL/CA-N	1
WL/MNOI (Tech. Library)	1
WL/MNSH	4

WL/FIES/SURVIAC
Wright Patterson AFB OH 45433-6553
1

HQ USAFE/INATW
APO NY 09012-5001
1

DARPA/TTO
Tactical Technology Office
Attn: Mr. Peter Kemmy
1400 Wilson Blvd.
Arlington VA 22209-2308
1

Naval Surface Weapons Center
Attn: Mr. P. T. Adams, Code G-35
Dahlgren VA 22448
1

SDIO/TNC
Attn: Mr. Mick Blackledge and
Maj Donna Stromecki
Washington DC 20301-7100
1

SDIO/TNI
Attn: Dr. Dwight Duston and
Lt Col Pedro Rustan
Washington DC 20301-7100
1

U.S. Army Strategic Defense Command
Attn: DASD-H-Q (Lt Col Steven Kee)
P.O. Box 1500
Huntsville AL 35807-3801
1

U.S. Army, ARDEC
SMCAR-FSE, Bldg 329
Attn: Mr. Tom Coradeschi and
Dr. Thaddeus Gora
Picatinny Arsenal NJ 07806-5000
1

U.S. Army Ballistic Research Laboratory
SLCBR-TB-EP
Attn: Dr. John Powell
Aberdeen Proving Ground MD 21005
1

WL/POOX
Attn: Dr. Charles E. Oberly
Wright Patterson AFB OH 45433-6553
1

Auburn Research Foundation
Office of the Vice Pres. for Research
Attn: Ms. Barbara Ausharian
202 Samford Hall
Auburn University AL 36849-5160
DAL: 29335; CCAL: 0001689
1
Route to Drs. R. F. Askew (Dir., Leach Nuclear Science Ctr.) and E. J. Clothiaus (Dept. of Physics)

GA Technologies, Inc.
Attn: Mr. Charles N. Stem
P.O. Box 85608
San Diego CA 92138
DAL: 06785; CCAL: 0002129
1
Route to Drs. Robert Bourque and L. Holland

General Dynamics Pomona Division
Attn: Ms. Dottie Patterson
1675 W. Mission Blvd.
Pomona CA 91769-2507
DAL: 01461; CCAL: 0001182
1
Route to Dr. Jaime Cuadros

Boeing Aerospace Company
Attn: Mr. David Wilson
P.O. Box 3999
Seattle WA 98124-2499
DAL: 27984; CCAL: 0005729
1
Route to Dr. J. E. Shrader

Electromagnetic Launch Research, Inc.
Attn: Mr. Thomas R. Fradette
2 Fox Rd.
Hudson MA 01749
DAL: 28861; CCAL: 0001587
1
Route to Drs. Henry Kolm and
Peter Mongeau and Mr. William Snow

IAP Research, Inc.
Attn: Mr. David P. Bauer
2763 Culver Ave.
Dayton OH 45429-3723
DAL: 28548; CCAL: 0000927
1
Route to Dr. John P. Barber

Lawrence Livermore Natl. Lab
Attn: Ms. Jean Higby
P.O. Box 808
Livermore CA 94550
DAL: 06635; CCAL: 0001362
1
Route to Dr. R. S. Hawke, L-156

Los Alamos Natl. Laboratory
Attn: Mr. Jack Carter, Report Librarian
P.O. Box 1633, MS-P364
Los Alamos NM 87545
DAL: 31455; CCAL: 0001652
1
Route to Drs. Jerry V. Parker and
L. A. Jones

LTV Aerospace and Defense Co.
Attn: Ms. Sherry D. Siler
P.O. Box 650003
Dallas TX 75265-0003
DAL: 00368; CCAL: 0000997
1
Route to Drs. Michael M. Tower and C. H.
Haight (M/S TH-83) and Mr. George L. Jackson

Maxwell Laboratories
Attn: Ms. Linda N. Thomas
8888 Balboa
San Diego CA 92123
DAL: 19248; CCAL: 0001705
1
Route to Drs. Rolf Dethlefson and
Ian McNab and Mr. Mark Wilkinson

General Research Corporation
Attn: Ms. Carol Donner
P.O. Box 6770
Santa Barbara CA 93160-6770
DAL: 10824; CCAL: 0000358
1
Route to Dr. William Isbell

GT Devices
Attn: Ms. Ada Burnette
5705 General Washington Dr.
Alexandria VA 22312
DAL: 29785; CCAL: 0001427
1
Route to Drs. Doug Witherspoon, Shyke
Goldstein, and Rodney L. Burton

NASA Lewis Research Center
Attn: L. T. Jarabek, Library
21000 Brookpark Rd.
Cleveland OH 44135
DAL: 00075; CCAL: 0007346
1
Route to Ms. Lynette Zana, MS 501-7

Pacific-Sierra Research Corp.
Attn: Ms. Celia A. Griffin
Suite 1100, 1401 Wilson Blvd.
Arlington VA 22209
DAL: 23323; CCAL: 0002150
1
Route to Dr. Gene E. McClellan

R&D Associates
Attn: Data Custodian
P.O. Box 92500
Los Angeles CA 90009
DAL: 12415; CCAL: 0001219
1
Route to Dr. Peter Turchi

SAIC Advanced Concepts Division
Attn: Ms. Bethany Madden
1519 Johnson Ferry Rd., Suite 300
Marietta GA 30062
DAL: 32383; CCAL: 0009775
1
Route to Dr. Jad Batteh and Messrs W. Smith
and L. Thornhill

SAIC
Attn: Mrs. Susan Deonarine
1427 N. Eglin Parkway
Shalimar FL 32579
DAL: 31327; CCAL: 0011312
1
Route to Mr. Floyd Graham and
Drs. Josh Kolawole, Glenn Rolader, and
Keith Jamison

MER Corporation
Attn: Data Custodian
7960 S. Kolb Rd.
Tucson AZ 85706
DAL: 31889; CCAL: 0003169
1
Route to Ms. Lori Leaskey and
Dr. R. Loutfy

SPARTA
Attn: Mr. James Poon
9466 Towne Centre Dr.
San Diego CA 92121-1964
DAL: 28397; CCAL: 0001185
1
Route to Dr. Michael M. Holland
and Mr. Stuart Rosenwasser

System Planning Corporation
Attn: Ms. Phyllis W. Moon
1500 Wilson Blvd.
Arlington VA 22209
DAL: 20874; CCAL: 0000279
1
Route to Mr. Donald E. Shaw

University of Alabama in Huntsville
Research Security Office
Attn: Ms. Gladys B. Jones
P.O. Box 18381
Huntsville AL 35804-8381
DAL: 28339; CCAL: 0002821
1
Route to Dr. C. H. Chen

University of Tennessee
Space Inst/Library
Attn: Ms. Marjorie Joseph
Tullahoma TN 37388-8897
DAL: 15965; CCAL 0000429
1
Route to Dr. Dennis Keefer

Sandia National Laboratory
Attn: Technical Library
P.O. Box 5800
Albuquerque NM 87185
DAL: 23683; CCAL: 0001104
1
Route to Drs. Maynard Cowan (Dept 1220)
and Jim Asay

University of Texas
Center for Electromechanics
Balcones Research Center
Attn: Ms. Marcie Powell
P.O. Box 200668
Austin TX 78720-0668
DAL: 00111; CCAL: 0005531
1
Route to Prof. William Weldon and
Mr. Raymond Zowarka

Westinghouse Elec. Corp, Marine Div.
Technical Library EE-5
Attn: Riet Blei
P.O. Box 3499
Sunnyvale CA 94088-3499
DAL: 06933; CCAL: 0000703
1
Route to Drs. Dan Omry and Hugh Calvin

Westinghouse Electric Co.
Science & Technology Center Library
Attn: Ms. Dee Hanko
1310 Beulah Rd.
Pittsburgh PA 15235
DAL: 00415; CCAL: 0000704
1
Route to Dr. Bruce Swanson

W. J. Schaffer Associates, Inc.
Attn: Data Custodian
321 Billerica Rd.
Chelmsford MA 01824-4191
DAL: 32309; CCAL: 0001458
1
Route to Dr. George I. Kachen